

# Strain Engineering of Ideal Rashba States on Layered Semiconductor Surface

Wenmei Ming,<sup>1</sup> Z. F. Wang,<sup>1</sup> Miao Zhou,<sup>1</sup> and Feng Liu<sup>1,\*</sup>

<sup>1</sup>*Department of Materials Science and Engineering, University of Utah, Salt Lake City, UT 84112*

Spin splitting of Rashba states in 2D electron systems provides a promising mechanism of spin manipulation for spintronics applications. Ideal Rashba states, which are separated in energy from spin-degenerated bulk states, have been so far shown to exist on polar semiconductor surface of BiTeX (X=I, Br and Cl) [Phys. Rev. Lett. **108**, 246802 (2012); *ibid.* **110**, 107204 (2013)], due to the underlying bulk properties of polarity and strong spin-orbit coupling (SOC). Using first-principles electronic structure and nonequilibrium Green's function transport calculations, here we demonstrate an alternative approach to realize ideal Rashba states by growing a Au single layer on the "strained" layered semiconductor  $\beta$ -InSe(0001). The Rashba states so formed are completely isolated in the substrate band gap and show a nearly perfect sinusoidal spin oscillation effect in transport. They originate from a mechanism different from BiTeX, that is, the Au overlayer provides the strong SOC while the interface gives rise to the polarization. Our approach may be generalized to other metal overlayers and layered semiconductor substrates, aided by strain engineering.

PACS numbers: 73.20.At 72.25.Mk 75.70.Tj 71.15.Mb

The Rashba effect refers [1] to spin splitting of 2D electronic states as a result of a perpendicular electric field in the presence of SOC. Much recent effort has been made in studying this effect in solid state systems for potential spintronics applications, such as spin field transistor [2] and intrinsic spin Hall effect [3]. The degree of spin splitting, quantified by the Rashba parameter  $\alpha$ , scales with the strength of electric field and SOC. The earliest realization of the Rashba effect was made in the asymmetric quantum well formed in InGaAs/InAlAs heterostructure [4], with small spin splitting. Nobel metal (e.g., Au [5], Ag [6] and Ir [7]) and *sp*-orbit heavy-metal surfaces (e.g., Bi [8], Sb [9] and Pb [10]) were shown to have large spin splitting. Heavy metal adatoms alloying with metal (e.g., Bi/Ag(111) [11]) and/or semiconductor surfaces (e.g., Si(111) [12]) were found to possess giant Rashba splitting. Most recently, new surface systems with Rashba splitting have been reported in graphene [13] and topological insulators [14–16]. However, because the substrates previously adopted are either metal or semiconductor with strong dangling bonds, typically Rashba surface states are overwhelmed by the large number of spin-degenerated substrate states, hindering their practical applicability.

There are two apparent conditions to realize large Rashba spin splitting: a large SOC and a large electric field. It has been recently demonstrated by both theory [17] and experiment [18] that these two conditions can be met by surface electronic states formed at the Te-terminated surface of bismuth tellurohalides, BiTeX (X = I, Br and Cl), a peculiar family of polar semiconductors. The Bi atoms provide the required large SOC, while the underlying polar semiconductor substrate provides a large electric field at the surface. Most significantly, the resulting Rashba states are situated completely inside the bulk band gap. Consequently, they are called ideal Rashba states, because they are separated

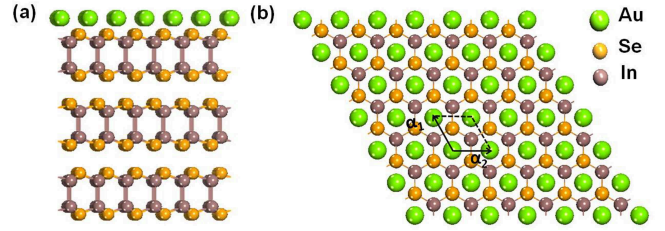


FIG. 1: (a) Side view of the (6 $\times$ 6) supercell structure of Au grown on layered InSe(0001) substrate, which is shown with only the top three layers for clarity. (b) Top view of the supercell.  $\alpha_1$  and  $\alpha_2$  represent the surface unit cell vectors.

in energy from the spin-degenerated bulk states, so that the surface transport of Rashba states is isolated from the bulk carrier contribution. In this Letter, based on first-principles electronic structure and nonequilibrium Green's function transport calculations, we demonstrate an alternative approach to realize ideal Rashba effect by strain engineered growth of a Au single layer on the layered large band-gap semiconductor  $\beta$ -InSe(0001) substrate. It exploits a physical mechanism different from BiTeX, with the Au overlayer providing the strong SOC and the Au/InSe(0001) interface giving rise to the polarization.

The bulk phase of  $\beta$ -InSe has a large band gap of 1.2 eV [19]. It has a layered crystal structure, with each layer consisting of Se-In-In-Se atomic planes and stacking along  $z$  direction. Within each layer, In and Se are bonded covalently; between layers, they are bonded with van der Waals (vdW) interaction. Its in-plane lattice constant is 4.05 $\text{\AA}$ . The atomic structure of Au/InSe(0001) is shown in Fig. 1(a-b) for side and top views, respectively. The first-principles calculation are carried out based on density function theory with projector augment wave pseudopotential [20] and Perdew-Burke-Ernzerhof [21]

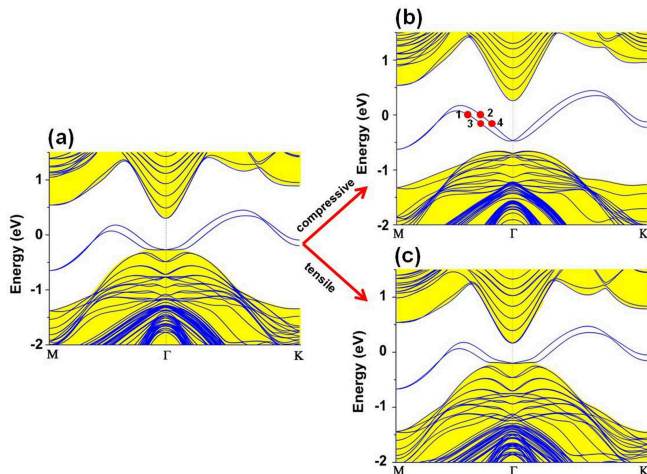


FIG. 2: Band structures of Au/InSe(0001) under different strain cases: (a) strain-free. (b) Compressive strain =  $-1.2\%$ . (c) Tensile strain =  $+1.2\%$ .

exchange-correlation functional using the VASP package [22]. All the atoms are allowed to relax until the forces are smaller than  $0.01 \text{ eV}/\text{\AA}$ .  $600 \text{ eV}$  kinetic energy cutoff and  $11 \times 11 \times 1$   $\Gamma$  centered k-mesh sampling are adopted for total energy convergence. The substrate is simulated by 7 layers of  $(1 \times 1)$ -InSe(0001) with an vacuum layer of more than  $20 \text{\AA}$ .

The interlayer binding energy between Au and InSe(0001) is  $\sim 0.5 \text{ eV}/\text{surface-unit-cell}$ . This indicates that the surface interaction is in an "intermediate" range [23], slightly stronger than the vdW bond but significantly weaker than the typical chemical bond. Fig. 2(a) shows the corresponding band structures of Au/InSe(0001) along  $M - \Gamma - K$  directions. The shaded area represents the substrate states and the two separate lines are the surface states, (whose location will be seen more clearly in the later discussion of charge distribution). Importantly, the two surface bands show a large Rashba spin splitting at the k-points from mid-point of  $M - \Gamma$  to mid-point of  $\Gamma - K$  and is mostly inside in the substrate band gap. Therefore, naturally by itself, this system can already significantly reduce the effect of substrate carriers, having two advantages: (1) the substrate has a large band gap; (2) on one hand, its surface interaction with Au is weak enough to avoid strong hybridization between the surface and substrate states; on the other hand, it is strong enough to induce a large Rashba spin splitting. However, in the vicinity of  $\Gamma$ , the Rashba surface bands are buried by the substrate states.

Next, we demonstrate by strain engineering the formation of "ideal" Rashba states from the Rashba surface bands above. We apply both compressive and tensile bi-

axial strains to the substrate to tune the relative position of the surface and the underlying substrate bands. Compressive strain is found to reduce the overlap between the surface and substrate bands, and the surface bands become situated completely inside the band gap of the substrate under a compressive strain of  $-1.2\%$ , as shown in Fig. 2(b). This can be attributed to the substrate band gap enlargement due to the down-shifting and up-shifting of the valence and conduction bands, respectively, relative to the surface bands. In contrast, tensile strain exerts an opposite effect that the overlap between the surface and substrate bands increases, and the band gap shrinks, with the up-shifting and down-shifting of the valence and conduction bands, respectively, as seen under a tensile strain of  $+1.2\%$  in Fig. 2(c). This tunable band positioning under strain indicates different deformation potentials for valence, conduction and the surface bands [24], respectively. In the following, all the results shown are for the ideal Rashba states engineered by a  $-1.2\%$  strain, corresponding to a strained lattice constant of  $\sim 4 \text{\AA}$ .

We have identified the asymmetric potential responsible for the Rashba spin splitting and the nonzero  $\alpha \propto \int \partial V(z)/\partial z dz$  [25]. The in-plane averaged potential  $V(z) = \frac{1}{A} \int V(x, y, z) dx dy$ , where  $A$  is the surface area, along  $z$  direction is shown in Fig. 3(a). The red dashed box indicates the region of Au and the first layer of the substrate, where electrons experience an asymmetric potential. In the remaining region, however, the potential is symmetric and almost identical for each layer to that in the bulk. This indicates that the Rashba states are localized only in the top Au+InSe layer. We further confirm this by calculating the local charge distribution for the Rashba states 1-4 as labeled in Fig. 2(b) at each atomic plane from the top-most Au to the bottom-most Se plane, as shown in Fig. 3(b-e). The red dashed boxes show that the charge of each state is mostly distributed in the first five atomic planes, beyond which it is negligibly small. An implication from this spatial localization of the Rashba states is that even a small thickness of substrate such as only one layer of InSe(0001) can be used to realize similar ideal Rashba states, which is a useful feature for producing strain in InSe(0001) grown on another substrate. Moreover, from tight-binding point of view, Rashba spin splitting originates from atomic Stark effect [26] under the potential-asymmetry-induced electric field and SOC, therefore the Rashba wavefunction must contain orbital compositions such as  $s/p_z$  and  $p_z/d_{z^2}$ , which have opposite parities in  $z$  direction to have nonzero Stark matrix elements. This is indeed confirmed by plotting orbital compositions of the Rashba states 1-4 in Fig. 3(f-i), which all contain large amount of  $s$ ,  $p_z$  and small amount of  $d_{z^2}^2$  components at each atomic plane.

Furthermore, we show the spin polarization texture of the Rashba states in Fig. 4. The spin polarization is defined:  $\vec{p}(\vec{k}) = [\langle S_x(\vec{k}) \rangle, \langle S_y(\vec{k}) \rangle, \langle S_z(\vec{k}) \rangle]$ ,

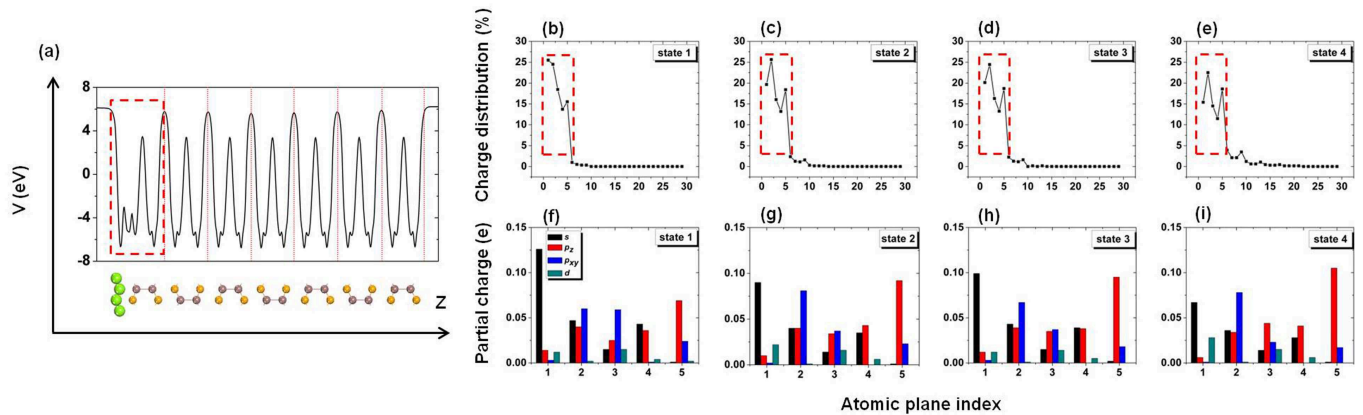


FIG. 3: (a) Plane-averaged potential  $V$  along  $z$ -axis. (b-e) Charge distribution of the Rashba states 1-4, as labeled in Fig. 2(b) as a function of atomic plane. (f-i) Orbital compositions in the first five atomic planes for the Rashba states 1-4.

where  $\langle S_\alpha(\vec{k}) \rangle = \langle \psi(\vec{k}) | \sigma_\alpha | \psi(\vec{k}) \rangle$ , ( $\alpha = x, y, z$ ). It is plotted at two iso-energy surfaces of  $E = 0.0$  eV and  $-0.12$  eV. Blue and red colors represent outer and inner branches of the Rashba bands, respectively. Overall, the iso-surface is isotropic for the inner circle with smaller  $k$ -vector, but gains some anisotropy of hexagonal shape for outer circle with larger  $k$ -vector. The  $z$ -component of the spin polarization is about ten times smaller than the  $x$ - and  $y$ - components, and the in-plane spin polarization is nearly perpendicular to the  $k$ -vector. This spin polarization texture is very similar to that in 2D Rashba SOC free-electron gas, which has only in-plane spin distribution [27]. Because the spin polarization texture reflects the  $k$ -dependent effective Rashba SOC magnetic field, the spin polarization of a spin-up electron injected into a free-electron gas channel with Rashba SOC was shown to oscillate sinusoidally over its travel length by spin-precession [28]. Hence, Au+InSe(0001) is expected to possess similar sinusoidal spin oscillation effect. Thus, we fit the Rashba bands to the free-electron Rashba band dispersion. The fitted Rashba parameter is  $0.45$  eV $\text{\AA}$ . It corresponds to a characteristic spin precession length [29]  $L_{so} (= (\frac{\pi}{\alpha})(\frac{\hbar^2}{2m}))$ , where  $m$  is the electron effective mass, of  $\sim 50$   $\text{\AA}$ , over which electron up-spin is rotated to down-spin, and that the periodicity of the sinusoidal oscillation is  $2L_{so} = \sim 100$   $\text{\AA}$ .

The spin-dependent electron conductance is calculated to reveal electron spin oscillation effect in Au/InSe(0001). From the wavefunctions of the Rashba bands of first-principle calculation, the maximally localized Wannier functions are constructed by using Wannier90 package [30]. The two Wannier functions obtained do not resemble any simple atomic orbitals, but hybridized orbitals with comparable distribution at both the top Au layer and the first layer of the InSe substrate. An effective tight-binding Hamiltonian of the Rashba bands is then obtained using the two Wannier functions as ba-

sis. A two-terminal nanoribbon device is constructed with the width of  $4a$  ( $a$  is the surface lattice constant of InSe(0001)), as shown in Fig. 5(a). The left lead is ferromagnetic and the right lead is nonmagnetic. We assume no SOC in the lead regions by artificially setting the Hamiltonian matrix elements of the spin-flip term to zero, and the channel region has the SOC as described by the full effective Hamiltonian. Fig. 5(b) shows the band structure of the nanoribbon representing the channel region. The Fermi energy is chosen to be at the position indicated by the red dashed line, crossing only two bands with Rashba splitting. The small width of the device gives rise to a transverse confinement potential, so that the spin-degenerate states, which are seen in Fig. 2 around Brillouin-zone corner (e.g.,  $M$  and  $K$ ), do not appear around the Fermi energy, leaving only the bands with Rashba SOC. On the other hand, our further calculation shows that significant increase of the ribbon width eventually brings down those spin-degenerate states to the same energy window of the Rashba bands, which should be avoided.

The conductance  $G(E_F)$  of the device is calculated using nonequilibrium Green's function method and Landauer-Büttiker formalism [31]:

$$G_{pq}(E_F) = \frac{e^2}{h} \text{Tr}(\Gamma_{lp} G^R \Gamma_{rq} G^A), \quad (1)$$

where  $G^R = G^{A+}$  is retarded Green function of the channel,  $\Gamma$  describes the interface coupling between the lead and the channel, and  $p, q$  are spin indexes. In Fig. 5(c),  $G_{\uparrow\uparrow}(E_F)$  and  $G_{\uparrow\downarrow}(E_F)$  are plotted for the spin-up and spin-down contributions to the total conductance, respectively, as a function of channel length ( $L$ ). They both exhibit nearly perfect sinusoidal oscillation with periodicity of  $\sim 90a$  ( $\sim 360$   $\text{\AA}$ ). This oscillation periodicity from the nanoribbon configuration is  $\sim 4$  times as large as that estimated from the 2D configuration. We confirm

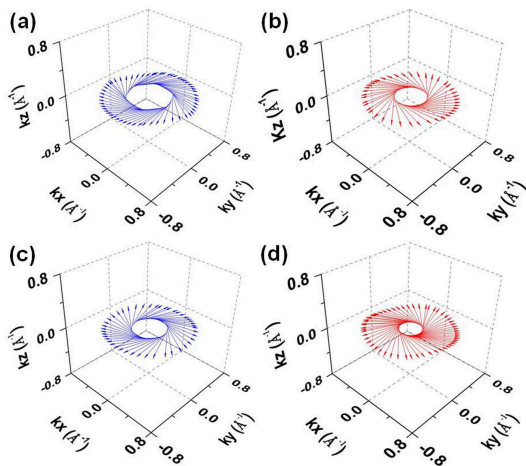


FIG. 4: Spin polarization textures of the Rashba bands at two iso-energy surfaces of  $E = 0.0$  eV (a-b) and  $E = -0.12$  eV (c-d), respectively.

this increased oscillation periodicity by again fitting the nanoribbon band structure to free-electron Rashba band dispersion. We find that the Rashba parameter  $\alpha$  is reduced to  $\sim 0.25$  eV $\text{\AA}$  and the effective mass  $m$  is reduced to be about half of that for 2D configuration. Therefore the oscillation periodicity  $2L_{so}$  is increased by  $\sim 4$  times, which is consistent with the increase from the conductance calculation. The change of  $\alpha$  and  $m$  is originated from the interplay between the comparable strengths of transverse potential confinement and Rashba SOC in the channel, which results in finite interband mixing and consequent modified Rashba band dispersion, as studied before in Ref. [28, 32].

Lastly, we point out that the compressive strain, which is critical for realizing the ideal Rashba bands in Au/InSe(0001), can be achieved by epitaxially growing InSe(0001) thin film on a semiconductor substrate with smaller lattice constant. Several substrates can be chosen such as GaAs(111), AlAs(111), ZnSe(111) and Ge(111), which all have surface lattice constant  $\sim 4$   $\text{\AA}$ , and hence impose the desired amount of strain on InSe(0001) thin film. On the other hand, InSe(0001) can be replaced by other layered semiconductor substrates such as those from metal chalcogenides family [33], and they may also exhibit ideal Rashba states upon heavy metal deposition.

In conclusion, we have demonstrated the formation of ideal Rashba states by strain engineering of heavy-metal film on layered large band-gap semiconductor substrate. The first-principle band structure calculation of Au single layer on strained InSe(0001) has shown that the Rashba bands with large spin-splitting are situated completely inside the substrate band gap. It originates from a physical mechanism different from BiTeX, that is, the Au overlayer provides the strong SOC while the interface gives rise to the polarization. The sinusoidal spin oscillation

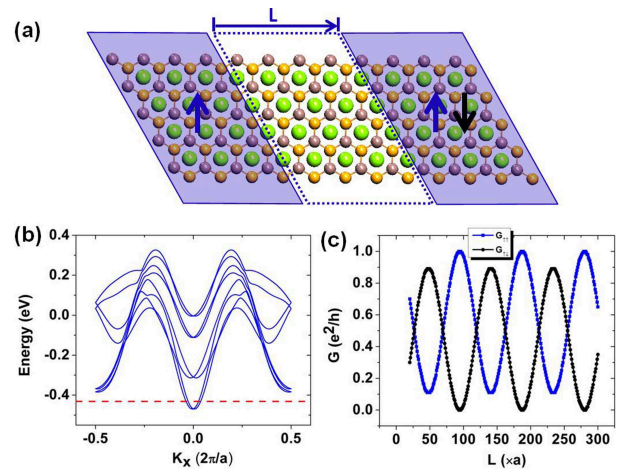


FIG. 5: (a) Two-terminal device setup: the boxes on the left and on the right represent source and drain leads without SOC, respectively. The left lead is ferromagnetic and the right lead is nonmagnetic. The middle dashed-line box represents the channel with Rashba SOC. (b) Band structure of the channel when assuming periodic structure in transport direction ( $L$ ). The red dashed line shows the Fermi energy position used in the conductance calculation. (c) The spin-up  $G_{\uparrow}(E_F)$  and spin-down  $G_{\downarrow}(E_F)$  contributions to the total conductance, as a function of device length ( $L$ ).

effect is confirmed by the conductance calculation with nonequilibrium Green's function method. Our approach may be generalized to other metal overlayers and layered semiconductor substrates, which is useful to reduce the unwanted effect of substrate spin degenerate carriers on spintronics devices

W. M. and Z. F. were supported by NSF MRSEC (Grant No. DMR-1121252); M. Z and F. L. were supported by DOE-BES (Grant No. DE-FG02-04ER46148). We thank the CHPC at University of Utah and NERSC for providing the computing resources.

\* Corresponding author. E-mail: fliu@eng.utah.edu

- [1] E.I. Rashba, Sov. Phys. Solid State **2**, 1109 (1960); Y.A Bychkov and E.I. Rashba, JETP Lett. **39**, 78 (1984).
- [2] S. Datta, and B. Das, Appl. Phys. Lett. **56**, 665 (1990).
- [3] Jairo Sinova, Dimitrie Culcer, Q. Niu, N. A. Sinitsyn, T. Jungwirth, and A. H. MacDonald, Phys. Rev. Lett. **92**, 126603 (2004).
- [4] JunSaku Nitta, Tatsushi Akazaki, and Hideaki Takayanagi, Phys. Rev. Lett. **78**, 1335 (1997).
- [5] S. LaShell, B. A. McDougall, and E. Jensen, Phys. Rev. Lett. **77**, 3419 (1996).
- [6] D. Popovic, F. Reinert, S. Hufner, V. G. Grigoryan, M. Springborg, H. Cercellier, Y. Fagot-Revurat, B. Kierren and D. Malterre, Phys. Rev. B **72**, 045419 (2005).
- [7] A. Varykhalov, D. Marchenko, M. R. Scholz, E. D. L. Rienks, T. K. Kim, G. Bihlmayer, J. Sanchez-Barriga,

- and O. Rader, Phys. Rev. Lett. **108**, 066804 (2012).
- [8] Yu. M. Koroteev, G. Bihlmayer, J. E. Gayone, E. V. Chulkov, S. Blugel, P. M. Echenique, and Ph. Hofmann, Phys. Rev. Lett. **93**, 046403 (2004).
- [9] K. Sugawara, T. Sato, S. Souma, T. Takahashi, M. Arai, and T. Sasaki, Phys. Rev. Lett. **96**, 046411 (2006).
- [10] J. Hugo Dil, Fabian Meier, Jorge Lobo-Checa, Luc Patthey, Gustav Bihlmayer, and Jurg Osterwalder, Phys. Rev. Lett. **101**, 266802 (2008).
- [11] Christian R. Ast, Jurgen Henk, Arthur Ernst, Luca Moreschini, Mihaela C. Falub, Daniela Pacile, Patrick Bruno, Klaus Kern, and Macro Grioni, Phys. Rev. Lett. **98**, 186807 (2007).
- [12] I. Gierz, T. Suzuki, E. Frantzeskakis, S. Pons, S. Ostanin, A. Ernst, J. Henk, M. Grioni, K. Kern, and C. R. Ast, Phys. Rev. Lett. **103**, 046803 (2009).
- [13] Yu. S. Dedkov, M. Fonin, U. Rudiger and C. Laubschat, Phys. Rev. Lett. **100**, 107602 (2008).
- [14] Jin-Jian Zhou, Wanxiang Feng, Ying Zhang, Shengyuan A. Yang and Yugui Yao, Sci. Rep. **4**, 3841 (2014).
- [15] P. D. C. King, R. C. Hatch, M. Bianchi, R. Ovsyannikov, C. Lupulescu, G. Landolt, B. Slomski, J. H. Dil, D. Guan, J. L. Mi *et al.*, Phys. Rev. Lett. **107**, 096802 (2011).
- [16] Z.-H. Zhu, G. Levy, B. Ludbrook, C. N. Veenstra, J. A. Rosen, R. Comin, D. Wong, P. Dosanjh, A. Ubaldini, P. Syers, N. P. Butch, J. Paglione, I. S. Elfimov and A. Damascelli, Phys. Rev. Lett. **107**, 186405 (2011).
- [17] S. V. Eremeev, I. A. Nechaev, Yu. M. Koroteev, P. M. Echenique and E. V. Chulkov, Phys. Rev. Lett. **108**, 246802 (2012).
- [18] . M. Sakano, M. S. Bahramy, A. Katayama, T. Shimojima, H. Murakawa, Y. Kaneko, W. Malaeb, S. Shin, K. Ono, H. Kumigashira *et al.* Phys. Rev. Lett. **110**, 107204 (2013).
- [19] P. Gomes da Costa, R. G. Dandrea, R. F. Wallis and M. Balkanski, Phys. Rev. B **48**, 14135 (1993).
- [20] G. Kresse and D. Joubert, Phys. Rev. B **59**, 1758 (1999).
- [21] J. P. Perdew, K. Burke, and M. Ernzerhof, Phys. Rev. Lett. **77**, 3865 (1996).
- [22] G. Kresse and J. Furthmüller, Comput. Mat. Sci. **6**, 15(1996).
- [23] Z. Liu, C.-X. Liu, Y.-S. Wu, W.-H. Duan, Feng Liu, and J. Wu, Phys. Rev. Lett. **107**, 136805 (2011).
- [24] Miao Zhou, Zheng Liu, Zhengfei Wang, Zhaoqiang Bai, Yuanping Feng, Max G. Lagally and Feng Liu, Phys. Rev. Lett. **111**, 246801 (2013).
- [25] Miki Nagano, Ayaka Kodama, T Shishidou and T Oguchi, J. Phys.: Condens. Matter **21**, 064239 (2009).
- [26] Hongki Min, J. E. Hill, N. A. Sinitsyn, B. R. Sahu, Leonard Kleinman and A. H. MacDonald, Phys. Rev. B **74**, 165310 (2006); Sergej Konschuh, Martin Gmitra, and Jaroslav Fabian, *ibid* **82**, 245412 (2010); K. V. Shanavas, Z. S. Popovic and S. Satpathy, *ibid* **90** 165108 (2014).
- [27] Oleg Krupin, PhD dissertation "Dichroism and Rashba effect at magnetic crystal surfaces of rare-earth metals", Freie Universität Berlin, 2004.
- [28] Francisco Mireles and George Kirczenow, Phys. Rev. B, **64**, 024426 (2001).
- [29] Ming-Hao Liu, Son-Hsien Chen and Ching-Ray Chang, Phys. Rev. B **78**, 195413 (2008).
- [30] Ivo Souza, Nicola Marzari and David Vanderbilt, Phys. Rev. B, **65**, 035109 (2001).
- [31] Z. F. Wang and Feng Liu, Appl. Phys. Lett. **99**, 042110 (2011).
- [32] A. V. Moroz and C. H. W. Barnes, Phys. Rev. B, **60**, 14272 (1999).
- [33] A. Aruchamy, *Photoelectrochemistry and Photovoltaics of Layered Semiconductors* (Kluwer Academic, Netherlands, 1992).